ISABE-2005-1041

Control of Laminar Separation Bubbles Using Instability Waves

Ulrich Rist, Kai Augustin
Institut für Aerodynamik und Gasdynamik
Universität Stuttgart, Pfaffenwaldring 21
70550 Stuttgart, Germany
rist@iag.uni-stuttgart.de

ABSTRACT

This paper presents detailed investigations related to active transition control in laminar separation bubbles. The investigations rely on direct numerical simulations based on the complete Navier-Stokes equations for a flat-plate boundary layer, such that the wall boundary layer is fully resolved. A laminar separation bubble is created by imposing a streamwise adverse pressure gradient at the free-stream boundary of the integration domain. Different steady and unsteady boundary layer disturbances are then introduced at a disturbance strip upstream of separation and their effects on the separation bubble are studied. It is shown that the size of the separated region can be controlled most efficiently by very small periodic oscillations, which lead to travelling instability waves that grow to large levels by the hydrodynamic instability of the flow. Indications for the preferred frequency of these waves can be obtained from linear stability theory, but since the problem is non-linear, only direct numerical simulations can really qualify or disqualify the predictions. Over all, it turns out that *unsteady* two- or three-dimensional disturbances have a stronger impact on the size of the bubble than steady disturbances, because they directly provide initial amplitudes for the laminar-turbulent transition mechanism.

NOMENCLATURE

Symbols

δ^*	[m]	displacement thickness
Θ	[m]	momentum thickness
$H = \delta^*/\Theta$	[−]	shape parameter
f	[Hz]	disturbance frequency
L	[m]	reference length
U_∞	[m/s]	free-stream velocity
v'	[m/s]	wall-normal disturbance amplitude at the wall
x	[m]	streamwise coordinate
y	[m]	wall-normal coordinate
z	[m]	spanwise coordinate
$Re^* = U_\infty \cdot \delta^*/\upsilon$	[−]	displacement-thickness Reynolds number
$Re_\Theta = U_\infty \cdot \Theta/\upsilon$	[−]	momentum-thickness Reynolds number
α	[−]	streamwise wave number
α_T	[°]	spreading angle of turbulence (conceptual)
$\beta = 2\pi f L/ U_\infty$	[−]	disturbance frequency
ϖ_z	[−]	time-averaged vorticity

Abbreviations

DNS	direct numerical simulation
(h/k)	mode of the frequency (index *h*) spanwise wavenumber spectrum (index *k*)
LSB	laminar separation bubble
LST	linear stability theory
R	re-attachment point
S	separation point
T	laminar-turbulent transition
2-d	two-dimensional
3-d	three-dimensional

INTRODUCTION

The occurrence of laminar separation and turbulent reattachment in a so-called laminar or transitional separation bubble is a typical problem for low to medium Reynolds-number aerodynamics, e.g. on aircraft wings or blades of turbo machines, where they lead to unwanted performance penalties. Laminar separation bubbles should hence be avoided using some means of control. So far, this has been achieved primarily by a 'cautious' design or by placing some kind of turbulence trips or vortex generators upstream of separation. However, these approaches cannot adapt themselves to changing operation conditions such that performance penalties may occur under off-design conditions. On the other hand, avoiding laminar separation bubbles by design sacrifices the maximal possible efficiency or adds extra weight and costs to a turbine because of extra blades which are needed to make the passage narrower in order to keep the flow attached.

Therefore, some active separation control methods have been proposed recently. Mostly, they consist of using vortex generator jets (e.g. [1]) which enforce an earlier transition of the flow to turbulence and hence an earlier re-attachment or no laminar separation at all using brute force. More recently periodically pulsed jets have been found to

increase the efficiency of such devices [2]. On the other hand, detailed low-pressure turbine cascade measurements have shown that laminar separation bubbles which periodically disappear and reappear under the influence of periodically passing wakes exert less dissipation loss on the cascade compared to the fully turbulent case. According to [3], this is due to periodically appearing "calmed regions" after destruction of the LSB by the passage of a turbulent wake, before the LSB reappears. Such findings confirm that active separation control has the potential to reduce dissipation losses in a LP turbine environment.

In the present work we investigate the possibility of using *small-amplitude,* local wall vibrations or suction and blowing to excite low-amplitude Tollmien-Schlichting-wave-like periodic boundary-layer disturbances which are amplified by the hydrodynamic instability of the laminar boundary layer such that they control transition in a typical laminar separation bubble. Originally intended for laminar separation bubbles in aerodynamic boundary layers (i.e. along external surfaces, like a wing), our simulation results should be equally valid for boundary layers in turbo machines because of very similar boundary layer thicknesses and shape parameters.

PHYSICAL MECHANISMS OF A TRANSITIONAL LAMINAR SEPARATION BUBBLE

Laminar boundary layers are preferable for applications where a low skin friction is desired. However, they are very sensitive to adverse pressure gradients, and they tend to separate much earlier than a turbulent boundary layer. Thus, in a typical aerodynamic context with a changeover from favourable to adverse pressure gradient, a region of laminar flow typically ends with a transitional LSB soon after the flow encounters the adverse pressure gradient. The separated flow leads to uncontrolled unsteadiness and an additional pressure drag penalty. Both are difficult to predict because of the sensitivity of the flow to small back-ground disturbances, which are usually unknown because they cannot be measured.
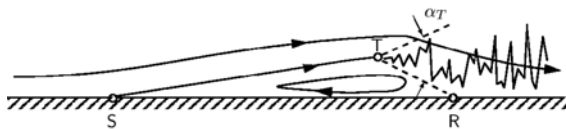
Fig. 1: Sketch of a transitional laminar separation bubble, S, T, and R: separation, transition, and re-attachment, resp.

The basic setup of a LSB is sketched in Fig. 1. The laminar boundary layer separates from the wall at a point 'S', transition to turbulence takes place at 'T', and the turbulent flow re-attaches at 'R'. The latter occurs because of an increased momentum exchange normal to the wall under the action of the larger turbulence eddies. With some oversimplification the re-attachment process can be thought to be due to a turbulent wedge that spreads at an angle

α_T from a point in the detached shear layer. The actual transition process starts by amplification of small-amplitude disturbances, which are already present in the upstream laminar flow or which are ingested from the free-stream via a process called 'receptivity'. Once large enough, higher frequencies occur and the shear layer disintegrates into structures of different size. For a more complete discussion of the laminar-turbulent transition process in LSBs see [4][5][6][7], for instance. Here, it is important to note that the position of 'T' within the bubble strongly depends on the initial disturbances. Since 'R' is related to the position of 'T' and the spreading angle α_T, the bubble length $(R - S)$ can be controlled by controlling the laminar-turbulent transition process, and it is the purpose of the present paper to present a detailed investigation of the underlying mechanisms. Therefore, the basic idea is to control laminar-turbulent transition by introducing small-amplitude disturbance waves upstream of the LSB. If these are in the unstable frequency range they will then grow to large amplitudes. The earlier they reach a certain level, the earlier laminar-turbulent transition and the earlier turbulent re-attachment of the flow that closes the bubble.

The paper is organized as follows. First the used numerical method is presented. Then a base flow is selected out of those studied in [8]. The linear instability of this is shown next using linear stability theory (LST) and comparisons with direct numerical simulations (DNS), followed by a demonstration of the influence of different forcing frequencies and disturbance amplitudes on the size of the LSB. A section based on 3-d simulations shows that obliquely travelling waves are an equally efficient means for control as 2-d waves and that *unsteady* forcing is much more efficient than steady 3-d forcing, e.g. via roughness elements. The paper ends with a summary and an outlook.

NUMERICAL METHOD

To study laminar separation bubbles multiple direct numerical simulations (DNS) of a flat-plate boundary layer have been performed. An adverse pressure gradient is applied locally at a given distance from the inflow at the free-stream boundary to force separation. The code used for the present DNS has been developed, verified and validated for the investigation of transitional boundary layers without and with separation, cf. [9]-[13].

Fig. 2 displays a sketch of the used integration domain together with a definition of the coordinates and the respective velocity components. All variables are non-dimensionalized with respect to the free-stream velocity U_∞ and a reference length L which leads to a reference Reynolds number Re given further down together with the results. The complete Navier-Stokes equations for incompressible flows are solved in a vorticity-velocity

formulation [9]. A fourth-order accurate numerical method is applied in time and space by finite differences in streamwise and wall-normal direction and by a four step explicit Runge-Kutta scheme in time [11]. For the spanwise direction a Fourier series implying periodic boundary conditions in that direction is used. Due to this the Poisson equations for the streamwise and spanwise velocity reduce to ordinary differential equations. The remaining 2-d Poisson equation for the wall-normal velocity is solved by a line relaxation method accelerated by a non-linear multi-grid algorithm, once the vorticity-transport equations have been advanced to the next Runge-Kutta step. All equations can be solved separately for each spanwise spectral mode k allowing effective parallelization.
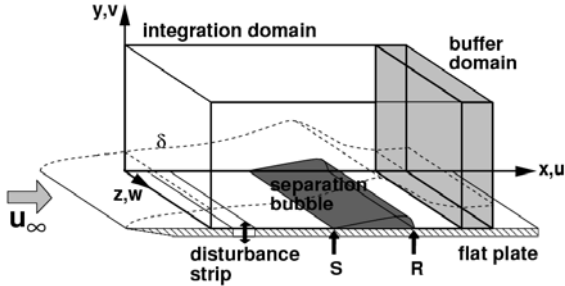
Fig. 2: Integration domain

At the inflow boundary a Blasius boundary layer solution with a momentum thickness Reynolds number $Re^* = U_\infty \delta^*/\upsilon = 1722$ is prescribed. At the surface of the plate the no-slip boundary condition is applied except for a disturbance strip upstream of the LSB where periodic 2-d and 3-d boundary layer disturbances are introduced into the flow by suction and blowing. The streamwise length of the disturbance strip has been set to one wavelength of the most amplified disturbance mode according to linear stability theory (LST) and the beginning is located approximately two wavelengths downstream of the inflow boundary. For the total streamwise length of the integration domain *18.41* wavelengths have been used, and the height of the domain corresponds to *16* boundary-layer displacement thicknesses at the inflow. To avoid non-physical reflections at the outflow boundary the disturbance amplitudes are artificially damped in a buffer domain by several orders of magnitude, using the method described in [10].

The laminar separation bubble is induced by a local deceleration of the 'potential' free-stream velocity imposed via the *u*-component at the upper boundary. Because of Bernoulli's equation this corresponds to imposing an adverse pressure gradient. The displacement effects of the LSB on the potential flow are captured by a viscous-inviscid boundary layer interaction model at every time step of the calculation (cf. [14] and [15]). Thus, the characteristic "pressure plateau" in the *u*-velocity distribution with a constant velocity in the

upstream part of the separation bubble and a sharp velocity drop in the region of transition and re-attachment develops during the calculation (see next section).

NUMERICAL RESULTS

Three different streamwise velocity drops have been investigated in [8]: one with 10%, one with 20%, and one with 25% reduction of free-stream velocity, where 10% means a reduction from $U/U_\infty = 1$ to $U/U_\infty = 0.9$, for instance. A comparison of the three is performed in Fig. 3 in terms of the "potential velocity" U_P, the resulting velocity U_M at the free-stream boundary, and in terms of the separation streamline $\Psi = 0$. Clearly, a larger velocity drop leads to a larger adverse pressure gradient and hence earlier separation at the wall. Also, the height of the bubble increases with rising pressure gradient. In all cases the typical "pressure plateau" develops in the velocity U_M (thick lines) as a result of the implemented viscous-inviscid interaction [14]. Here and in the following, dimensions are normalized with respect to a reference length L and the free-stream velocity U_∞ which yields $Re_L = L\,U_\infty\,/\upsilon = 10^5$.
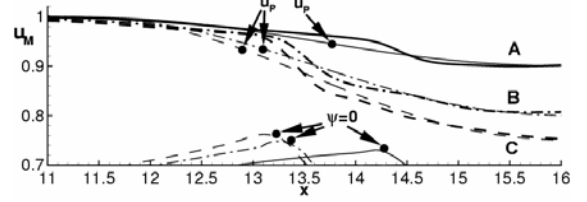
Fig. 3: Comparison of prescribed potential flow (thin lines) with resulting free-stream velocity (thick lines) and separation streamlines for the three base flows with 10% (A, ———), 20% (B, $- \cdot - \cdot -$) and 25% velocity drop (C, $- \ - \ -$)

In the following, "case A" will be considered only, because LSB control works in a similar manner in all three cases [8], as well as in those studied already earlier [16], [17].

Linear Instability of the Flow

Using velocity profiles $U(y)$ extracted at $x = const$ from the base flow obtained via DNS a linear stability analysis can be performed based on the Orr-Sommerfeld equation (cf. [18]). This analysis yields for a given x, Re, and frequency β complex streamwise wave numbers α whose imaginary part α_i is called the amplification rate. Integrating α_i versus x for fixed β leads to the disturbance amplification ratio $A/A_0 = e^{-\int \alpha_i dx}$, where A_0 is the initial amplitude. Fig. 4 presents results of such an analysis for base flow A and $A_0 = 10^{-6}$. The region of amplified disturbance frequencies is marked by increasingly dark shading. If the frequency is chosen correctly, e.g. between $\beta = 2.5$ and $\beta = 5$ a dramatic amplitude increase by 10^4 is observed for

the region shown. In contrast to what one might presume, the strong amplification starts well upstream of laminar separation (S) and is not just an indication of an inviscid "Kelvin-Helmholtz" instability. To make full use of these facts, the optimal disturbance generator placement should not be at the separation point but well upstream of this, i.e. in the region $x < 12$ for the present case.
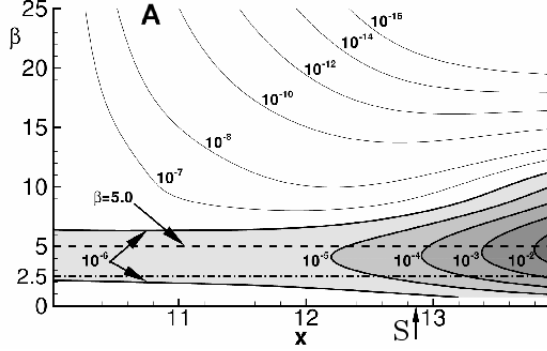
Fig. 4: Stability diagram for base-flow A according to linear stability theory

Verification in 2-d Simulations

The findings of the previous paragraph will now be checked using two-dimensional DNS. Primary parameters for the specification of 2-d disturbances at the upstream disturbance strip are the wall-normal suction and blowing amplitude v' (non-dimensionalized w.r.t. U_∞) and the forcing frequency $\beta = 2\pi f L/U_\infty$, where f is the frequency in Hertz. The range of amplified frequencies observed in Fig. 4 is rather narrow and should be obeyed for an efficient bubble control strategy, as already mentioned above. For the following simulations the frequency $\beta = 5$, indicated by the dashed line in Fig. 4, is chosen. A comparison of the obtained amplitude amplification with according LST results is shown in Fig. 5. The lines depict the maxima of the wall-parallel velocity disturbance component u' for the fundamental mode (1/0) and its higher harmonic (2/0), where (h/k) designates modes in the frequency (index h) spanwise wave number (index k) spectrum. The dash-dotted lines are results of LST for $\beta = 5$ and $\beta = 10$ (with symbols) shown for comparisons with and validation of the DNS.

Upstream of the disturbance strip (at $x \approx 11$) the fundamental disturbance amplitude decays to zero while the downstream growth corresponds over a large extent to the one predicted by LST. Since the higher harmonic is generated as a product of the fundamental with itself, it amplifies faster than its according LST results (lines with squares). Overall, both disturbances grow over several orders of magnitude until non-linear saturation which correlates with the formation of vortices in Fig. 6 further down. At vortex shedding the fundamental amplitude and its higher harmonic remain quasi constant. The point of non-linear amplitude saturation corresponds to point 'T' in the idealized sketch of Fig. 1.
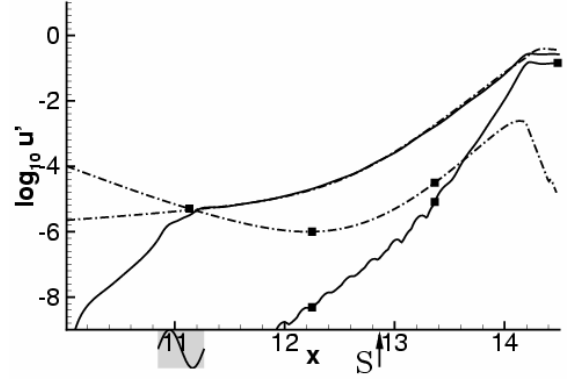
Fig. 5: Comparison of the growth of the fundamental disturbance (1/0) and its first harmonic (2/0) (marked with ■) with LST (dash-dotted lines)

Here, the reader should remind that laminar-turbulent transition and its influence on the laminar separation bubble are both non-linear phenomena and that their prediction needs a full (non-linear) simulation, i.e. linear theory can only give a somewhat limited insight into the useful parameter range. It cannot predict laminar-turbulent transition and its impact on the bubble size. This is why the higher harmonic doesn't behave according to LST. In addition, once the bubble has become smaller the linear instability of the flow is somewhat reduced. Nevertheless, most of the disturbance growth follows linear instability closely and LST can be used to estimate the effect of choosing different forcing frequencies. In addition, LST helps to explain the initial mechanisms. Thus, the investigation of the *non-linear* effects of unsteady forcing on the laminar separation bubble can so far only be investigated by full DNS.

As an illustration, results of one such simulation (frequency $\beta = 5$ and amplitude $v' = 10^{-6}$) are shown in Fig. 6 in terms of the instantaneous vorticity ω_z and the time-averaged separation streamline. The location and extend of the disturbance strip is again marked by a box at $x \approx 11.0$. The shear layer detaches from the surface at 'S' and reattaches at 'R' in the time mean. Downstream of the LSB a very high wall shear develops which resembles the high wall shear of a turbulent boundary layer despite the fact that only two-dimensional simulations have been performed here, and that a rather regular vortex shedding occurs in Fig. 6 due to the periodic forcing with a single frequency. It turned out that the wall-normal momentum transfer induced by these vortices mimics the turbulent transport to a large extend. For instance, the shape parameter of the present boundary layer after re-attachment is close to $H = 2.0$ while the one for a turbulent boundary layer is $H = 1.4 - 1.5$. Inside the present bubble the shape factor rises to $H \approx 7$. Upstream of $x \approx 13$ the disturbances are too weak to be seen in Fig. 6. This is why a logarithmic scale has been used in Fig. 5.
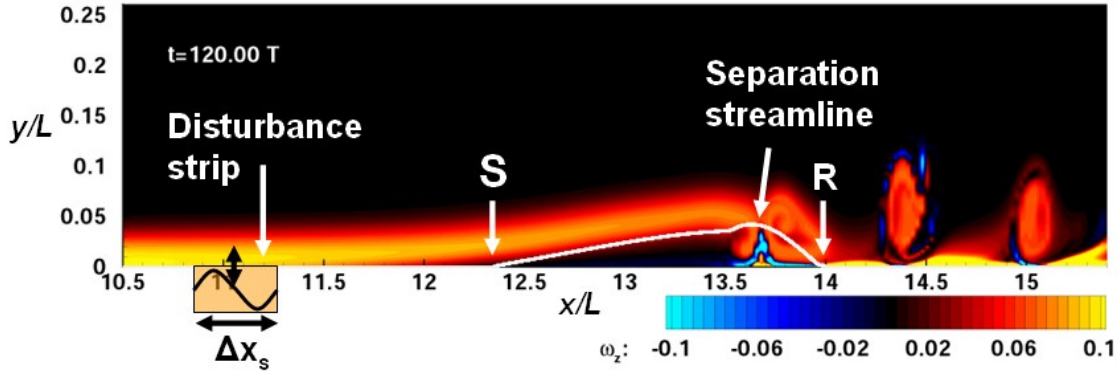
Fig. 6: Comparison of instantaneous vorticity with time averaged separation streamline and placement of disturbance strip

Effect of Disturbance Frequency

Results of LST in Fig. 4 have indicated the frequency band necessary for an efficient control. Two possible discrete frequencies have been indicated by horizontal lines there. Fig. 7 presents results for the lower disturbance frequency $\beta = 2.5$ in comparison with according LST results and the fundamental $\beta = 5$ from the previous case (dash-dotted line). A striking difference to Fig. 5 is that the higher harmonic ($\beta = 5$) lies also within the unstable region such that its growth agrees to an equally large extend with LST as the growth of the fundamental.

However, compared to the earlier case the fundamental of the present case (solid lines) grows somewhat slower after $x = 13$ such that non-linear saturation of the disturbances (T^*) occurs farther downstream than in the first case (T). Since the position of re-attachment is related to T, there is later re-attachment (large arrow at $x \approx 15$) compared to the first case (small arrow), such that the laminar separation bubble becomes larger. Interestingly, the point of laminar separation moves upstream at the same time (large vs. small arrow), an effect already observed earlier [5].
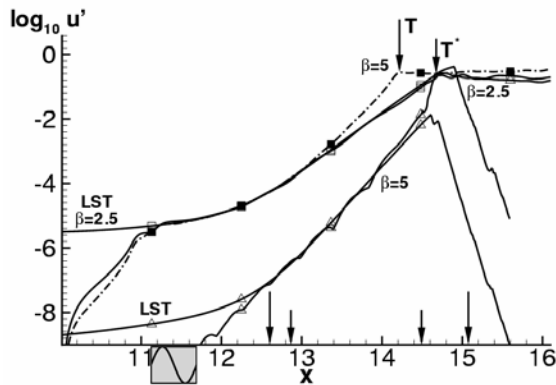
Fig. 7: Fundamental and higher harmonic disturbance growth for forcing with $\beta = 2.5$ compared to $\beta = 5$ (dash-dotted line) and LST

Thus, despite the same forcing amplitude and identical initial growth of the disturbances in the two cases, bubbles of different size develop. This is emphasized by means of the two separation streamlines in Fig. 8. It turns out that the larger of the two disturbance frequencies is more efficient for LSB control, because it produces earlier laminar-turbulent transition and a smaller bubble.
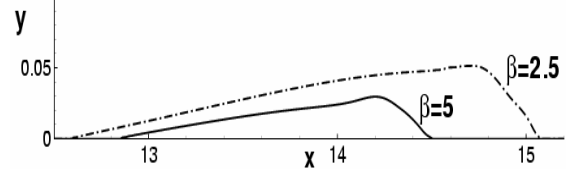
Fig. 8: Comparison of separation streamlines for forcing with $v' = 10^{-6}$ and two different frequencies

Effect of Increasing Disturbance Amplitudes

The disturbance amplitudes v' of the fundamental mode (1/0) $\beta = 5$ have been successively increased to find the relation between bubble size and forcing amplitude and to see whether the bubble can be made to completely disappear in the limit. The according bubbles are compared in Fig. 9. Indeed, there is a continuous reduction in bubble height, a downstream shift of 'S', and an upstream shift of 'R' as the forcing amplitude is increased from 10^{-6} to $2 \cdot 10^{-4}$.
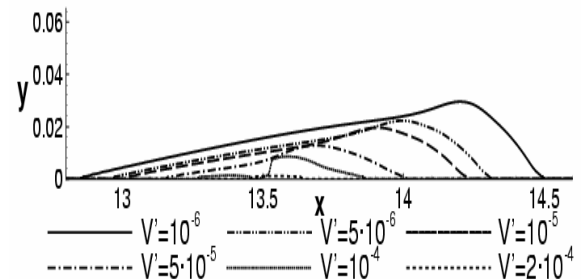
Fig. 9: Separation streamlines for increasing forcing amplitudes

Since the instability of the base flow decreases, once the size of the LSB gets smaller, the additional energy input to influence the LSB increases in a non-linear manner. Initially, the relation between bubble size and forcing amplitude is exponential as can be seen from an evaluation of the separation-

and re-attachment-point positions versus forcing amplitude *v'*, as well as the bubble length in Fig. 10.
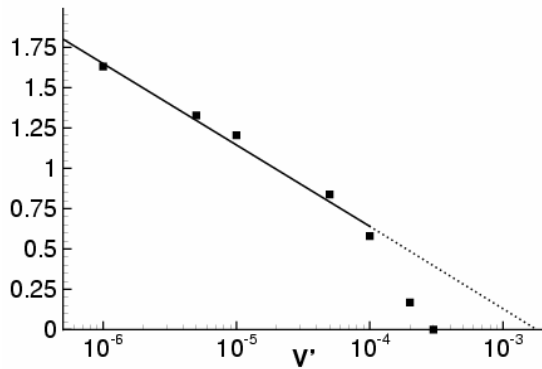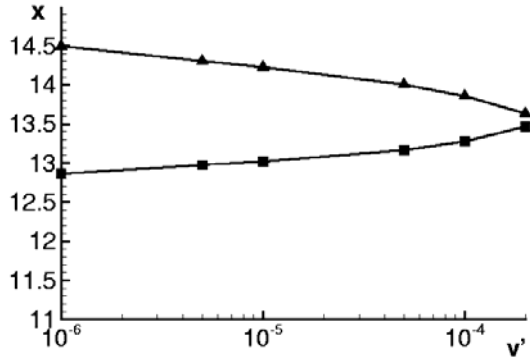
Fig. 10: Evolution of separation position (■)and re-attachment position (▲) with disturbance amplitude *v'* (top); evolution of bubble length (bottom)

The differences between the various cases are quite dramatic as illustrated in Fig. 11 by a comparison of the streamwise velocity profiles near the re-attachment position of the smallest bubble. The profile of the unforced case is shown as a solid line.
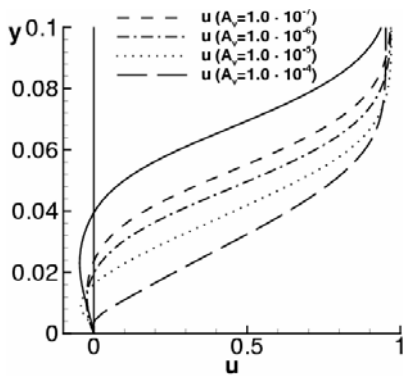
Fig. 11: Mean-flow velocity profiles at *x = 13.85* for the cases with different forcing amplitudes

Integral boundary-layer parameters of the cases with smallest and largest forcing, i.e. largest bubble and no bubble, are compared in Fig. 12. There is a three-fold increase of displacement thickness over the bubble and a two-fold increase of momentum thickness. When the bubble is suppressed both

parameters increase to a lesser extend. Since a larger momentum thickness is indicative of more drag according to v. Karman's integral momentum equation, it turns out that reducing the LSB must lead to a drag reduction.
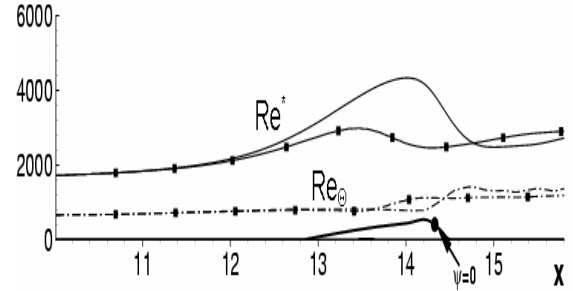
Fig. 12: Influence of forcing amplitudes (*v' = 10^{-6}* and *v' = 2·10^{-4}*, no symbols and symbols, resp.) on displacement and momentum thickness Reynolds numbers (solid and dash-dotted lines, resp.)

Effects of Three-Dimensional Forcing

Since 3-d disturbances can be generated much easier in practice than perfect 2-d ones, one has to consider the efficiency of using 3-d disturbances for laminar separation bubble control, as well. This is done now by adding a 3-d forcing to the fundamental 2-d case from the previous figures. The forcing of the 2-d fundamental is now denoted by *(1/0)* in the frequency spanwise wavenumber spectrum *(h/k)*. Its amplitude *v'* is kept at its previous level of *10^{-6}*, while the 3-d mode *(1/1)* is initially forced at a 10-times larger level *v' = 10^{-5}*. Here, the fundamental spanwise wavenumber *k* is set to *5.4596* which corresponds to a spanwise wavelength of $\lambda_z = 1.15$ and an angle of obliqueness of $\phi = 20^o$ relative to the free-stream direction. Adding this disturbance is equivalent to adding a pair of oblique waves *(1/±1)* because of spanwise symmetry imposed by the Fourier ansatz in *z*.

The disturbance amplification in Fig. 13 indicates now that mode *(1/1)* dominates the whole process with the consequence that 3-d higher harmonics grow to large levels, i.e. turbulence sets in much earlier now with according consequences on the separation bubble and its boundary layer parameters. These latter are illustrated in Fig. 14 by comparing the case with increased 3-d forcing *(1/1)*, identified with symbols, with the reference case from above.

The reaction of the flow to the oblique waves is comparable to a 10-fold increase of the 2-d forcing: The length of the laminar separation bubble decreases, and so does its height. Shape parameters and Reynolds numbers show an according difference. Because of a nearly identical growth of the 3-d disturbance *(1/1)* in comparison with the 2-d *(1/0)* the laminar separation bubble can be controlled by either of the two at practically the same efficiency. However, downstream of the bubble the full 3-d case delivers a flow that resembles a fully turbulent

boundary layer better than in the reference case, because of a lower shape factor.
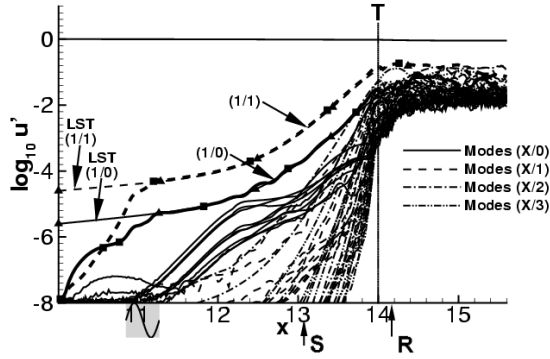
Fig. 13: Disturbance amplification for increased 3-d forcing at $v' = 10^{-5}$
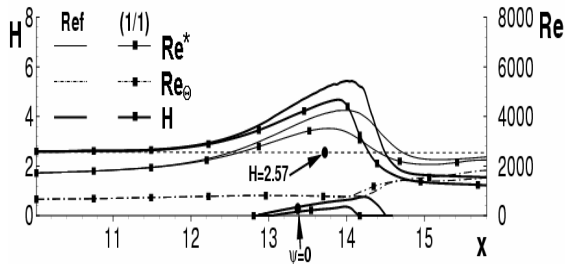
Fig. 14: Comparison of boundary layer parameters for increased 3-d forcing (1/1) with 2-d forcing (Ref)

Steady vs. Unsteady Three-Dimensional Forcing

The next investigation will now show the effect of using a *steady* 3-d forcing to control the bubble. Such an approach is closer to "more traditional" techniques, like applying a row of small bumps upstream of separation that cause turbulence in order to prevent laminar separation. For this investigation the spanwise wavenumber has been increased to *15* which corresponds to a spanwise wave length of *0.4189* in the present scaling. To simulate such a steady 3-d 'roughness', mode *(0/1)* has been forced with $v' = 10^{-3}$ in addition to the other modes in the reference case from above.

The resulting disturbance growth of individual modes is shown in Fig. 15. Initially, the spectrum is dominated by the steady 3-d mode and its higher harmonics *(0/k)*, but in contrast to the travelling ones, these are only moderately amplified. More on the amplification of steady modes in a flow with LSB can be found in [19].

Apparently, the laminar-turbulent transition process is not much affected by the additional steady disturbance, despite its large initial amplitude. This can be explained by the fact, that adding a steady roughness doesn't directly produce turbulence (which is inherently unsteady). The latter can only occur when wall-roughness interacts with fluctuations of the free stream. Hence, in practice, large roughness is needed to cause laminar-turbulent transition via some bypass-mechanism, i.e. one without linear amplification of disturbances

(in contrast to the driving mechanism in the present investigations).
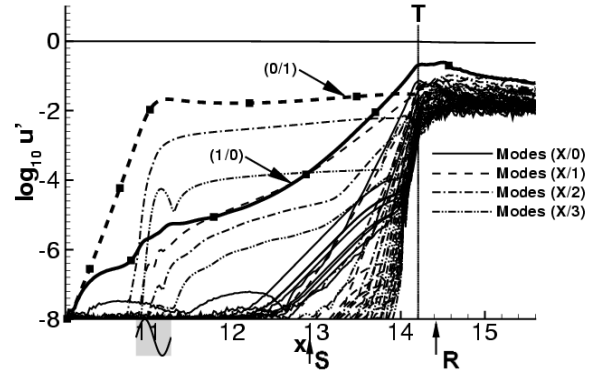
Fig. 15: Disturbance amplification under the influence of a steady 3-d disturbance (0/1)

In accordance with the above discussion the boundary layer parameters in Fig. 16 show that the effect of the steady 3-d forcing is decent, despite the *1000-fold* larger amplitude compared to the 2-d unsteady forcing above! The bubble shapes and the evolution of Reynolds numbers and shape factors remain practically unaltered.
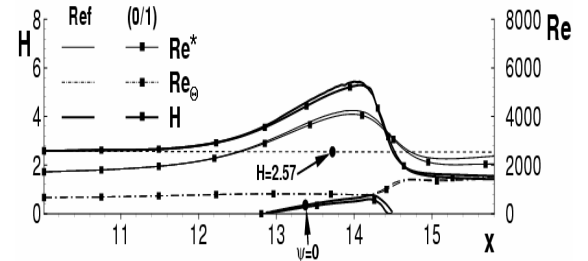
Fig. 16: Comparison of boundary layer parameters for large-amplitude steady 3-d forcing (0/1) with the reference case (Ref)

A visualisation of the 3-d separation surface (i.e. an approximation of the surface that separates the time-averaged recirculating flow inside the bubble from the external stream) shows that the steady 3-d disturbance amplitude was indeed considerably large such that it causes longitudinal grooves in the bubble (Fig. 17). Its inefficiency is hence not caused by a too small amplitude!
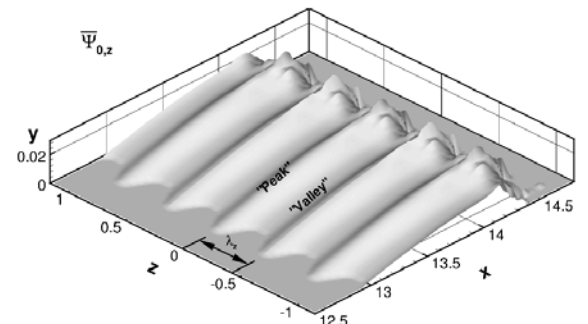
Fig. 17: Separation stream surface in case of large-amplitude steady 3-d forcing

CONCLUSIONS AND OUTLOOK

The above results show the advantages of the excitation of unsteady 2-d or 3-d disturbances with respect to "more traditional" approaches which rely on steady forcing. In order to provide the necessary unsteady disturbance amplitude, a possible control system for LSBs would consist of a frequency generator, an amplifier and an actuator, as already discussed in [16], mainly because it suffices to provoke laminar-turbulent transition by some appropriate means without an urgent need for some highly sophisticated controller. In fact, a simple switch that turns LSB control on or off when appropriate could be sufficient, once the different flow situations are understood well enough. As also shown in [16], the frequency generator could be replaced by a feed-back of instantaneous skin friction signals obtained from a position downstream of the separation bubble. The broad band of frequencies in the most unstable frequency range due to hydrodynamic instability then provides a robust signal source for the actuator, after an appropriate reduction to lower amplitudes. In a further step, distributed skin-friction sensors could be devised to detect the separation length via time-averaged skin-friction signals, which in turn could be used to control the feed-back amplitude gain, and hence the bubble.

In summary, it has been shown that separation bubbles can be significantly reduced in size and finally removed very economically by low-amplitude boundary layer disturbances, at least for the aerodynamic configurations investigated so far. Because of a good agreement of boundary-layer parameters with those found in LP turbines, and because of the excellent reproduction of such flows in a flat-plate boundary layer (see [3], for instance) it is expected that the present concept is equally valid in a turbo machine environment as in the laminar-flow airfoil context, where it was initially intended for.

REFERENCES

[1] J.P. Bons, R. Sondergaard, R.B. Rivir: Control of low-pressure turbine separation using vortex generator jets, AIAA-99-0367, 1999.

[2] J.P. Bons, R. Sondergaard, R.B. Rivir: Turbine separation control using pulsed vortex generator jets, transactions of the ASME 198 / Vol. 123, April 2001.

[3] R.D. Stieger and H.P. Hodson. Unsteady dissipation measurements on a flat pate subject to wake passing, Proc. Instn Mech. Engrs. Vol. **217** Part A, 413-420, 2003.

[4] A.V. Dovgal, V.V. Kozlov, A. Michalke, Laminar boundary layer separation: instability and associated phenomena, Progr. Aerospace Sci. **30**, 61-94, 1994.

[5] U. Rist, Zur Instabilität und Transition in laminaren Ablöseblasen. Habilitation, Universität Stuttgart, Shaker Verlag, 1999.

[6] U. Rist, On instabilities and transition in laminar separation bubbles, Proc. CEAS Aerospace Aerodynamics Research Conference, 10 - 12 June 2002, Cambridge, UK.

[7] U. Rist, Instability and transition mechanisms in laminar separation bubbles, VKI-LS *"Low Reynolds Number Aerodynamics on Aircraft Including Applications in Emerging UAV Technology"*, Rhode-Saint-Genèse, Belgium, 24-28 November 2003.

[8] K. Augustin, Zur aktiven Beeinflussung von laminaren Ablöseblasen mittels Grenzschichtstörungen, Dissertation Universität Stuttgart, 2005.

[9] U. Rist, H. Fasel, Direct numerical simulation of controlled transition in a flat-plate boundary layer. J. Fluid Mech. **298**, 211-248, 1995.

[10] M. Kloker, U. Konzelmann, H. Fasel, Outflow boundary conditions for spatial Navier-Stokes numerical simulations of transition boundary layers. AIAA Journal **31** (4), 620-628, 1993.

[11] M. Kloker, A robust high-resolution split-type compact FD scheme for spatial direct numerical simulations of boundary layer transition. Applied Scientific Research **59** (4), 353-377, 1998.

[12] U. Rist, U. Maucher, S. Wagner, Direct numerical simulation of some fundamental problems related to transition in laminar separation bubbles. In Computational Methods in Applied Sciences '96, ECCOMAS Paris, France, John Wiley & Sons Ltd., 319-325, 1996.

[13] U. Rist, U. Maucher, Investigations of time-growing instabilities in laminar separation bubbles. European Journal of Mechanics B/Fluids 21, 495-509, 2002.

[14] U. Maucher, U. Rist, and S. Wagner. Refined interaction method for direct numerical simulation of transition in separation bubbles. AIAA Journal, **38**(8):1385-1393, 2000.

[15] U. Maucher, Numerische Untersuchungen zur Transition in der laminaren Ablöseblase einer Tragflügelgrenzschicht, Dissertation Universität Stuttgart, 2002.

[16] K. Augustin, U. Rist, and S. Wagner. Investigation of 2d and 3d boundary layer disturbances for active control of laminar separation bubbles. AIAA 2003-0613, 2003.

[17] K. Augustin, U. Rist, S. Wagner, Active control of a laminar separation bubble, *in* P. Thiede (Ed.), *Aerodynamic Drag Reduction Technologies,* Proc. CEAS/DragNet Conference, Potsdam, 19.-21.6.2000, NNFM **76**, Springer-Verlag, Berlin, Heidelberg, 297-303, 2001.

[18] H. Reed, W.S. Saric, D. Arnal, Linear stability theory applied to boundary layers. Ann. Rev. Fluid Mech. **28**, 389-428, 1996.

[19] O. Marxen, U. Rist, S. Wagner, Effect of spanwise-modulated disturbances on transition in a separated boundary layer, AIAA Journal **42** (8), 937-944, 2004.